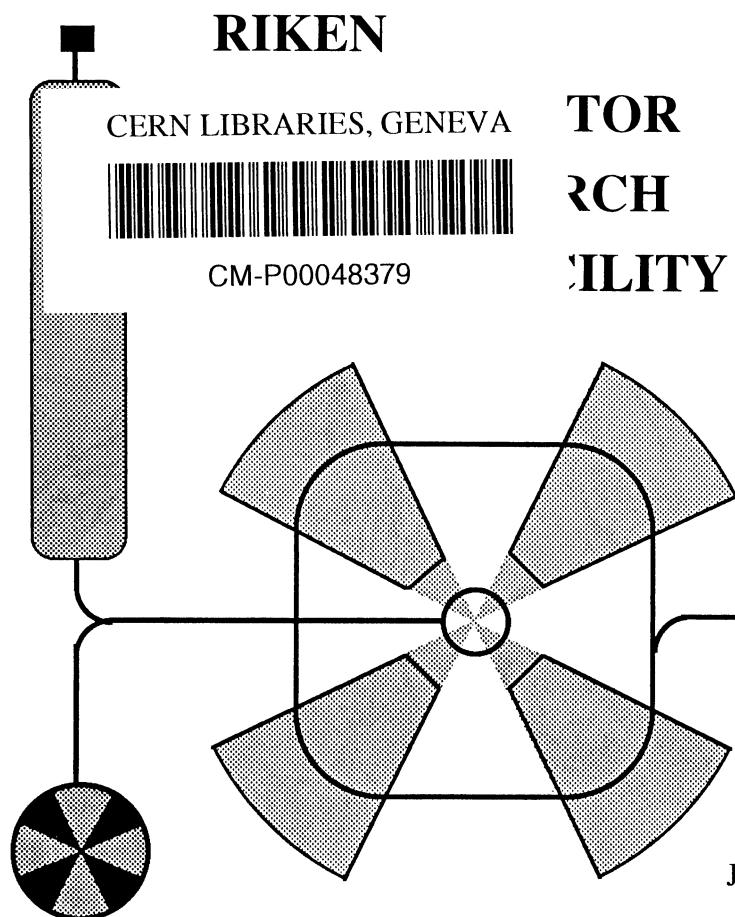


ISSN 1346-244X
RIKEN-AF-NP-427

**Isovector Quadrupole Resonance observed in
the $^{60}\text{Ni}(^{13}\text{C}, ^{13}\text{N})^{60}\text{Co}$ reaction at $E/A = 100$ MeV**

T Ichihara, M Ishihara, H Ohnuma, T Niizeki, Y Satou,
H Okamura, S Kubono, M Tanaka, and Y Fuchi



June 2002

The Institute of Physical and Chemical Research (RIKEN)
2-1 Hirosawa, Wako, Saitama 351-0198, Japan
TEL (048)462-1111 FAX (048)462-4642
e-mail *username@rikvax.riken.go.jp*

Isvector Quadrupole Resonance observed in the $^{60}\text{Ni}(^{13}\text{C},^{13}\text{N})^{60}\text{Co}$ reaction at $E/A = 100$ MeV

T Ichihara,^{1,*} M Ishihara,¹ H Ohnuma,² T Niizeki,³ Y Satou,⁴
H Okamura,⁵ S Kubono,⁴ M Tanaka,⁶ and Y Fuchi⁶

¹*RIKEN, 2-1 Hirosawa, Wako, Saitama 351-0198, Japan*

²*Department of Physics, Chiba Institute of Technology, Chiba 275-0023, Japan*

³*Faculty of Home Economics, Tokyo Kasei University, Tokyo 173-8602, Japan*

⁴*CNS, University of Tokyo, Tokyo 113-0033, Japan*

⁵*Department of Physics, Saitama University, Saitama 338-8570, Japan*

⁶*High Energy Accelerator Research Organization (KEK), Tsukuba 305-0801, Japan*

(Dated: June 10, 2002)

Abstract

Charge-exchange reaction $^{60}\text{Ni}(^{13}\text{C},^{13}\text{N})^{60}\text{Co}$ at $E/A = 100$ MeV has been studied to locate isovector ($\Delta T = 1$) non-spin-flip ($\Delta S = 0$) giant resonances. Besides the giant dipole resonance at $E_x = 8.7$ MeV, another resonance has been observed at $E_x = 20$ MeV with a width of 9 MeV. DWBA analysis on the angular distribution clearly indicated the $L = 2$ multipolarity, attributing the $E_x = 20$ MeV state to the giant isovector quadrupole resonance.

PACS numbers: 25.70.Kk, 24.30.Cz, 25.70.Bc, 27.50.+e

Giant resonances (GR) represent major modes of collective motion, which dictate the dynamical properties of nuclei. For a nucleus as a many-body system of nucleons, various multipole modes exist reflecting isospin (T) and spin (S) degrees of freedom. The isoscalar ($\Delta T = 0$) and isovector ($\Delta T = 1$) modes represent oscillations in which protons and neutrons move in phase and in opposite phase, respectively, while electric ($\Delta S = 0$) and magnetic ($\Delta S = 1$) modes correspond to non-spin-flip and spin-flip excitations, respectively. Among the isovector non-spin-flip modes, the dipole resonance (IVGDR, $L = 1$) is a classical example of the giant resonance, which has been explored most extensively and is known to prevail over the nuclear chart. On the other hand, only limited information has been so far obtained for the monopole (IVGMR; $L = 0$) and quadrupole resonances (IVGQR, $L = 2$) [1].

These two modes are supposed to be coherent states of $1p$ - $1h$ excitations across two major shells ($2\hbar\omega$), while the IVGDR is related to excitations of one major shell ($1\hbar\omega$). Accordingly the IVGMR and IVGQR are expected to appear at similar excitation energies, which are considerably higher than $82 A^{-1/3}$ MeV expected for the IVGDR. At such higher energies, the excitation spectrum becomes progressively complex with mixed contributions from various excitation modes on top of the mounting continuum background. The broader width of the resonance further increases the difficulty. These features have hampered unambiguous identification of the high-lying resonances.

In recent years, several attempts have been made to locate these high-lying resonances by employing charge-exchange reactions. Among those studies, measurements with reactions of (π^- , π^0) at 165 MeV [2], and (${}^7\text{Li}$, ${}^7\text{Be}$) at $E/A = 65$ MeV [3] provided strong indications for the existence of the IVGMR. On the other hand, clear observation of an IVGQR has been so far unsuccessful, while its occurrence was suggested from the forward-backward asymmetry due to the E1-E2 interference in (γ , n) and (n, γ) reactions [4], and by the multipole decomposition analysis of the inelastic electron scattering [5].

In this paper we report on the first clear identification of the IVGQR in the ${}^{60}\text{Ni}({}^{13}\text{C}, {}^{13}\text{N}){}^{60}\text{Co}$ reaction at $E/A = 100$ MeV. For comparison, a measurement on the (${}^{12}\text{C}$, ${}^{12}\text{N}$) reaction was also performed. These heavy ion reactions afford several advantages in probing the giant resonances of interest. First of all, they exhibit strong selectivity for $\Delta T = 1$ and $\Delta T_z = 1$ excitations, uniquely populating the isovector $T + 1$ resonances. As for

the spin selectivity, the ($^{13}\text{C}, ^{13}\text{N}$) reaction allows $\Delta S = 0, 1$ excitations while the ($^{12}\text{C}, ^{12}\text{N}$) reaction only allows $\Delta S = 1$ excitations. For the former reaction, it is also known that $\Delta S = 0$ components are much more favored than $\Delta S = 1$ components because of its large Fermi matrix element ($M_F/M_{GT} \sim 5$) [6]. Hence the combination of these two reactions could provide a useful means to distinguish between spin-flip and non-spin-flip modes.

There exist earlier measurements on the ($^{13}\text{C}, ^{13}\text{N}$) reaction performed at $E/A = 50$ MeV [6]. However the observed angular distributions turned out to be rather structureless, disallowing L determination for the resonances. This is thought to be due to considerable contributions of multi-step processes at these energies. In contrast, it has been shown for the ($^{12}\text{C}, ^{12}\text{N}$) reaction that such contributions become almost negligible in the higher energy domain of $E/A \geq 100$ MeV [7, 8].

Given all these favorable features, the high-energy ($^{13}\text{C}, ^{13}\text{N}$) reaction can be expected to make a powerful tool to locate the $\Delta S = 0$ and $\Delta T = 1$ resonances. Indeed, the present measurement has revealed a clear $L = 2$ peak of ^{60}Co , which is uniquely attributed to the IVGQR.

The measurements were performed using $E/A = 100$ MeV ^{13}C and $E/A = 135$ MeV ^{12}C beams from the K540 RIKEN Ring Cyclotron and spectrograph SMART [9] with a QQDQD-configuration. The elastic scattering was also measured for the ^{13}C beam. A self-supporting enriched ^{60}Ni target of 3.0 mg/cm² was used, resulting in an overall energy resolution of 1 MeV. The spectrograph had a large angular acceptance of 200 mr for vertical and 50 mr for horizontal planes, which covered an angular range from -5.7° to 5.7° at a time by injecting the beam at 0° . The spectrograph was equipped with a pair of cathode readout drift chambers (CRDC) [10], which were located at the focal plane and separated from each other by 50 cm. Plastic scintillation counters placed behind the CRDC's provided ΔE and time of flight signals for particle identification. The momentum as well as the vertical and horizontal scattering angles were obtained by reconstructing the trajectory through the two CRDC's. The overall angular resolution achieved was estimated to be approximately 0.1° . Thus differential cross sections were obtained for every 0.2° bin of the scattering angle (lab) for the charge-exchange reactions and for 0.1° bins for the elastic scattering of $^{60}\text{Ni}(^{13}\text{C}, ^{13}\text{C})^{60}\text{Ni}$.

Figure 1 shows typical energy spectra of the $^{60}\text{Ni}(^{13}\text{C}, ^{13}\text{N})^{60}\text{Co}$ reaction at $E/A = 100$ MeV. Data at two angular bins, $\theta_{\text{lab}} = 0^\circ\text{-}0.2^\circ$ and $\theta_{\text{lab}} = 0.8^\circ\text{-}1.0^\circ$, are shown together

with the difference spectrum between these two bins. The excitation energies are given with respect to the ground state of ^{60}Co . The difference spectrum is also shown for the $^{60}\text{Ni}(^{12}\text{C}, ^{12}\text{N})^{60}\text{Co}$ reaction at $E/A = 135$ MeV for the sake of comparison.

Besides the low-energy peak from the $^1\text{H}(^{13}\text{C}, ^{13}\text{N})\text{n}$ reaction, the energy spectra are dominated by resonance structures built on top of large continuum background. The profiles of resonances are most clearly indicated in the difference spectra. The difference spectrum for $^{60}\text{Ni}(^{13}\text{C}, ^{13}\text{N})^{60}\text{Co}$ shows two resonances at $E_x = 8.7$ MeV and 20 MeV, while that for $^{60}\text{Ni}(^{12}\text{C}, ^{12}\text{N})^{60}\text{Co}$ shows a resonance at $E_x = 10$ MeV. The difference of the resonance structure between the two reactions can be attributed to the ΔS selectivity. In the $(^{12}\text{C}, ^{12}\text{N})$ reaction only $\Delta S = 1$ states will be excited. Hence the resonance at $E_x = 10$ MeV can be assigned to a $\Delta S = 1$ resonance. Indeed this resonance is consistent with the assignment of the spin dipole resonance [3, 11]. On the other hand, the $(^{13}\text{C}, ^{13}\text{N})$ reaction favors $\Delta S = 0$ excitations over $\Delta S = 1$ excitations [6]. Thus the two resonances at $E_x = 8.7$ MeV and 20 MeV may be assigned to be $\Delta S = 0$ states. The absence of these peaks in the $(^{12}\text{C}, ^{12}\text{N})$ spectrum supports this conclusion.

In order to extract yields of the observed resonances, subtraction of the continuum background is crucial. The origin of the background may be mainly attributed to the quasi-free charge-exchange reactions. In treating the continuum spectra, we followed the phenomenological expression developed by Erell *et al.* [2]. In this model, the functional form of the doubly differential cross section for the continuum background was given (Eq. (3.1) of Ref. [2]) as a product of a Lorentzian function of the ejectile energy E , which is centered at an energy E_{QF} and has a width W_L , and an energy cutoff function characterized by a maximum cutoff energy E_0 and a cutoff energy scale parameter T . We have assumed $E_{\text{QF}} = E_{\text{free}} - S_n$, where E_{free} is the energy of ^{13}N for the $\text{p}(^{13}\text{C}, ^{13}\text{N})\text{n}$ reaction and S_n is the neutron separation energy of ^{60}Co . The parameter E_0 was set at 0 MeV to accommodate the contributions from unresolved discrete levels as well as three-body continuum states.

Peak fitting procedure has been performed for the 20 spectra of the $^{60}\text{Ni}(^{13}\text{C}, ^{13}\text{N})^{60}\text{Co}$ reaction over the angular range from $\theta_{\text{lab}} = 0^\circ - 0.2^\circ$ bin to $\theta_{\text{lab}} = 3.8^\circ - 4.0^\circ$ bin. Peak shapes for $E_x = 8.7$ MeV and $E_x = 20$ MeV states were assumed to be Gaussian. The value of T was set to be same for the entire angular range while the angular dependence was introduced for W_L . After a systematic search we found that the parameter set of $W_L = 34(1.0 + 0.06\theta_{\text{lab}} + 0.06\theta_{\text{lab}}^2)$ MeV and $T = 15.5$ MeV reproduces the continuum

TABLE I: Excitation energies and widths of the resonances observed in $\Delta T_z = 1$ charge-exchange reactions leading to ^{60}Co

	$(1\hbar\omega)$		$(2\hbar\omega)$		Ref
	E_x (MeV)	Γ (MeV)	E_x (MeV)	Γ (MeV)	
(π^-, π^0)	10.7 ± 1.6	4.2 ± 2.0	22.4 ± 1.7	14.7 ± 2.1	[2]
$(^7\text{Li}, ^7\text{Be})$	8.5 ± 0.5	4.0 ± 0.5	20 ± 2	10 ± 2	[3]
$(^{13}\text{C}, ^{13}\text{N})$	9.1 ± 0.3	2.2 ± 0.4	22.1 ± 0.8	8.1 ± 1.0	[6]
Present work	8.7 ± 0.5	2.8 ± 0.8	20 ± 2	9 ± 2	

background consistently for all the angles involved ($\chi^2/f = 1.5$). For the sake of comparison, the peak fitting was also performed with a different E_0 value of 7.5 MeV, at which the three-body decay channel opens. The extracted angular distribution was hardly changed for the 20 MeV resonance.

Typical results from the fitting procedure are found in Fig. 1. The dashed curves show the calculated continuum spectra, which reproduce a large portion of the high energy spectra and well represent the overall feature of the background. The solid curves in Fig. 1, obtained by superposing the two Gaussian peaks of the resonances, reproduce the experimental data very well.

The energy and width (Γ) of the two resonances thus determined are listed in Table I together with the previous results on various (n,p) type exchange reactions on ^{60}Ni . All the measurements exhibited two prominent peaks at excitation energies in the neighborhood of 9 and 20 MeV. As for the lower-energy peak, the assignment of the IVGDR is consistently supported. On the other hand, there exist different possibilities for the higher-energy peak. While the works on the (π^-, π^0) [2], and $(^7\text{Li}, ^7\text{Be})$ [3] reactions claimed the $L = 0$ assignment, the work on the $(^{13}\text{C}, ^{13}\text{N})$ reaction at $E/A = 50$ MeV [6] was unable to confirm the $L = 0$ nature of the resonance. A recent self-consistent random phase approximation (RPA) calculation, which employs the Skyrme force SGII, indicates that the IVGQR strength of ^{60}Co is peaked around 23 MeV and that of the IVGMR around 26 MeV [12]. It is thus plausible that the IVGQR as well as the IVGMR gives rise to a high-energy peak as observed in the present work.

The extracted angular distributions for $E_x = 8.7$ MeV and $E_x = 20$ MeV states are

TABLE II: Optical potential parameters deduced from the $^{60}\text{Ni}(^{13}\text{C},^{13}\text{C})^{60}\text{Ni}$ reaction at $E/A = 100$ MeV

V_r (MeV)	r (fm)	a (fm)	W_r (MeV)	r_w (fm)	a_w (fm)
52.8	1.09	0.79	35.0	0.87	1.78

plotted in Fig. 2. They exhibit clear diffraction patterns, suggesting dominance of the one-step process at $E/A = 100$ MeV. In contrast, the angular distribution of the background shown together exhibits a smooth fall-off behavior.

In order to determine the multipolarity (L) of the resonances, microscopic DWBA calculations were performed using the code developed by Lenske [13]. Optical-potential parameters were determined by fitting the present data on the $^{60}\text{Ni}(^{13}\text{C},^{13}\text{C})^{60}\text{Ni}$ elastic scattering with the code ECIS79 [14]. They are summarized in Table II, and the calculated angular distribution is compared with the experiment in Fig. 3. In the DWBA calculations, the form factors of $L = 0, 1$ and 2 were obtained by folding the transition densities of the projectile and the target with the effective interaction [15]. The transition density of the projectile was obtained from the shell-model single-particle wave functions [7], while the transition density of the target was assumed to take a collective form of Tassie type [1, 16] with Wood-Saxon radial distribution of $r_0 = 1.2$ fm and $a = 0.6$ fm.

The solid curves in Fig. 2 represent the results of the DWBA calculations. They are obtained after folding the calculated results with experimental angular resolutions and by normalizing the absolute magnitudes to the experimental data. For the $E_x = 8.7$ MeV state, an IVGDR was assumed. Hence the $L = 1$ form factor was taken. Indeed, a very good fit has been obtained, justifying the validity of the DWBA analysis. For the $E_x = 20$ MeV state, we have studied two cases, one with the $L = 0$ IVGMR form factor and the other with the $L = 2$ IVGQR form factor. The calculated angular distribution for the $L = 0$ IVGMR (the dotted curve in Fig. 2) exhibits a steep rise at 0° and the first minimum near the $\theta_{\text{cm}} = 0.8^\circ$. However, these distinctive features are hardly manifested in the observed angular distribution. On the other hand, an excellent fit has been obtained with the calculated distribution for the $L = 2$ IVGQR excitation. This result strongly indicates that the resonance state observed at $E_x = 20$ MeV is an IVGQR rather than an IVGMR.

The present observation of the IVGQR raises a puzzling problem why the (^{13}C , ^{13}N) reaction favorably excites the IVGQR while other reactions such as (^7Li , ^7Be) reportedly populate only the IVGMR. In this respect, we have examined the radial overlap of the form factor with the penetrability profile of the probe particles. The insert of the Fig. 3 shows a comparison of the penetrability profiles of the present (^{13}C , ^{13}N) reaction at $E/A = 100$ MeV and (^7Li , ^7Be) at $E/A = 65$ MeV [3] using the optical potentials as employed in the relevant analyses. It was found that the former reaction is much more peripheral than the latter. On the other hand, the form factor for the IVGMR is mostly distributed in the interior of the nucleus while that for the IVGQR is shifted towards the surface region. Hence it is plausible that the excitation of the IVGQR is favored in the (^{13}C , ^{13}N) reaction while that of the IVGMR is favored in the (^7Li , ^7Be) reaction.

In summary, we have studied the $^{60}\text{Ni}(^{13}\text{C}, ^{13}\text{N})^{60}\text{Co}$ reaction at $E/A = 100$ MeV to observe isovector non-spin-flip giant resonances. Besides the IVGDR at $E_x = 8.7$ MeV, a significant peak was observed at $E_x = 20$ MeV with a width of 9 MeV. DWBA analysis of the observed angular distribution clearly indicates $L = 2$ multipolarity, revealing the occurrence of the IVGQR. No evidence of the IVGMR was observed by the present experiment.

We are grateful to Dr. I. Hamamoto and Dr. H. Sagawa for their stimulating discussions. Sincere thanks are expressed to Dr. G. Colò for providing us with the results of his RPA calculation.

* Electronic address: ichihara@riken.go.jp

- [1] M. N. Harakeh and A. van der Woude, *Giant Resonances* (Oxford University Press, 2001)
- [2] A. Erell *et al.*, *Phys. Rev. C* **34**, 1822 (1986)
- [3] S. Nakayama *et al.*, *Phys. Rev. Lett.* **83**, 690 (1999)
- [4] D. A. Sims *et al.*, *Phys. Rev. C* **55**, 1288 (1997)
- [5] Y. Torizuka *et al.*, *Phys. Rev. C* **11**, 1174 (1975)
- [6] C. Bérat *et al.*, *Nucl. Phys.* **A555** 455 (1993)
- [7] T. Ichihara *et al.*, *Phys. Lett. B* **323** 278 (1994); *Nucl. Phys.* **A577** 93c (1994); **A583** 109c (1995)
- [8] H. Lenske *et al.*, *Phys. Rev. Lett.* **62** 1457 (1989)

- [9] T Ichihara *et al* , Nucl Phys **A569** 287c (1994)
- [10] M H Tanaka *et al* , Nucl Instrum Methods **A362** 521 (1995)
- [11] A L Williams *et al* , Phys Rev C **51** 1144 (1995)
- [12] G Colò, (private communications); see also, G Colò and N Van Giai, Phys Rev C **53** 2201 (1996)
- [13] H Lenske, Nucl Phys **A482** 343c (1988)
- [14] J Raynal, code ECIS79, (unpublished)
- [15] M A Franey and W G Love, Phys Rev C **31** 488 (1985)
- [16] L J Tassie, Aust J Phys **9** 407 (1956)

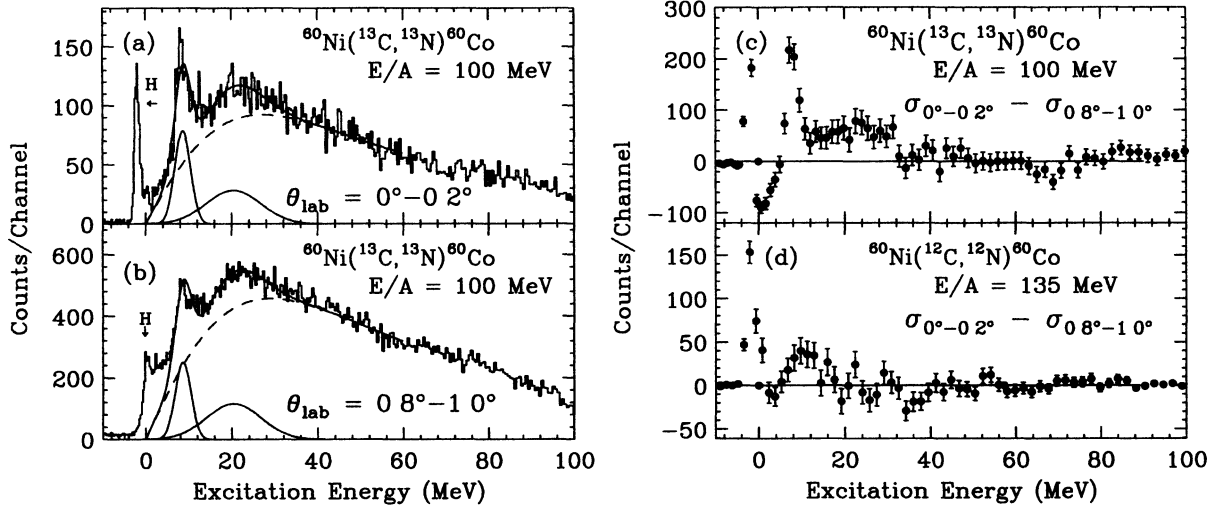


FIG 1: Energy spectra of the $^{60}\text{Ni}(^{13}\text{C}, ^{13}\text{N})^{60}\text{Co}$ reaction at $E/A = 100$ MeV for the angular bins of (a) $\theta_{\text{lab}} = 0^\circ\text{-}0.2^\circ$ and (b) $\theta_{\text{lab}} = 0.8^\circ\text{-}1.0^\circ$. The symbol H indicates the $^1\text{H}(^{13}\text{C}, ^{13}\text{N})\text{n}$ reaction owing to the target contamination. (c) represents the difference spectrum obtained by subtracting (b) from (a) after renormalization (every 4-channels are packed in a bin for better statistics). (d) represents the difference spectrum obtained for the $^{60}\text{Ni}(^{12}\text{C}, ^{12}\text{N})^{60}\text{Co}$ reaction at $E/A = 135$ MeV.

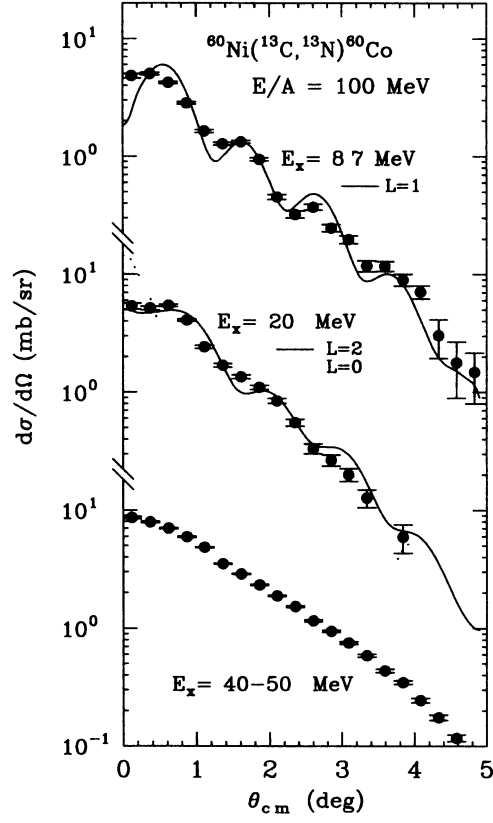


FIG 2: Differential cross sections for the $E_x = 8.7$ MeV and $E_x = 20$ MeV states and the background sum of $E_x = 40-50$ MeV of the $^{60}\text{Ni}(^{13}\text{C}, ^{13}\text{N})^{60}\text{Co}$ reaction at $E/A = 100$ MeV. Error bars represent only statistical ones. Curves are obtained from DWBA calculations. The solid curve for $E_x = 8.7$ MeV is calculated assuming the IVGDR ($L = 1$). The solid and dotted curves for $E_x = 20$ MeV are calculated assuming the IVGQR ($L = 2$) and IVGMR ($L = 0$), respectively.

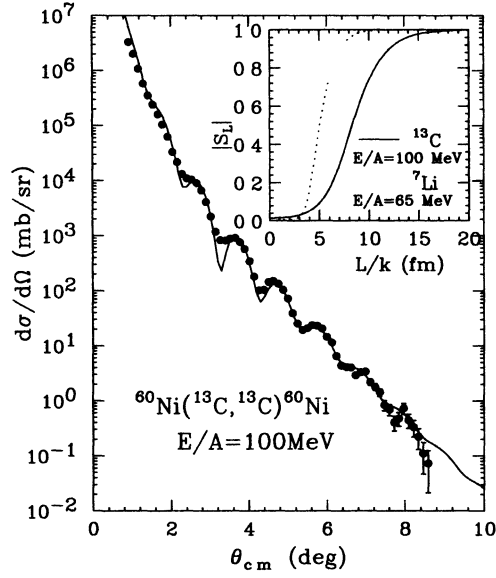


FIG 3: Measured differential cross sections for the elastic scattering of ^{13}C from ^{60}Ni at $E/A = 100$ MeV. The solid curve is calculated with the optical parameters in Table II folded by the experimental angular resolution. The solid and dotted curves of the insert show the absolute values of the S-matrix elements (S_L) calculated for the $^{60}\text{Ni}(^{13}\text{C}, ^{13}\text{C})^{60}\text{Ni}$ reaction at $E/A = 100$ MeV and $^{60}\text{Ni}(^7\text{Li}, ^7\text{Li})^{60}\text{Ni}$ reaction at $E/A = 65$ MeV (Ref [3]), respectively. The horizontal axis is the orbital angular momentum (L) divided by the wave number (k) and given in units of fm.